

Crossband Flexible UWB Multiple Access for High-Rate Multipiconet WPANs

Liuqing Yang, *Member, IEEE*, and Georgios B. Giannakis, *Fellow, IEEE*

Abstract—Emerging indoor technologies including wireless multimedia and personal area networks (WPANs) entail high-rate systems capable of supporting multiple users (piconets) with variable rates. These requirements motivate the design of multiband (MB) ultra-wideband (UWB) radios for their simplicity in handling pronounced frequency selectivity, agility in coping with interference, scalability in providing multirate operation, and their potentially low cost. Relative to baseband UWB radios, MB-UWB systems have gained popularity in the IEEE standards for short-range wireless links. However, multiple-access (MA) schemes must be designed carefully to harness the diversity benefits provided by the MB-UWB propagation, in a spectrally efficient manner. To this end, we introduce a crossband flexible UWB MA scheme for multipiconet WPANs. The resultant design that we term FLEX-UWB offers resilience to multiuser interference, can conveniently accommodate various spreading alternatives, enables full multipath diversity, and can effect scalable spectral efficiency (from low to medium and high data rates). Simulations confirm the merits of FLEX-UWB radios in comparison with various alternatives.

Index Terms—Multiband (MB), multicarrier (MC), multiple access (MA), ultra-wideband (UWB), wireless personal area networks (WPANs).

I. INTRODUCTION

AS A WIRELESS technology promising enhanced user capacity at potentially ultra-high data rates, ultra-wideband (UWB) radios have experienced about ten years of evolution. Shortly after the first UWB radios appeared [15], time-hopping (TH) spreading codes were advocated to enable multiple access (MA) in low-duty-cycle impulse radio (IR) UWB systems [10], [12]. Later on, direct-sequence (DS) and hybrid DS-TH alternatives were proposed to facilitate IR-MA [7], [11] and fully exploit the large processing gain inherent to IR-UWB systems

Paper approved by M. Zorzi, the Editor for Multiple Access of the IEEE Communications Society. Manuscript received April 25, 2005; revised December 31, 2005 and March 23, 2006. This work was prepared through collaborative participation in the Communications and Networks Consortium sponsored by the U. S. Army Research Laboratory under the Collaborative Technology Alliance Program, Cooperative Agreement DAAD19-01-2-0011. The U.S. Government is authorized to reproduce and distribute reprints for Government purposes notwithstanding any copyright notation thereon. This work was also supported in part by the National Science Foundation under Grants EIA-0324864 and CNS-0420836. This paper was presented in part at the Asilomar Conference on Signals, Systems, and Computers, Monterey, CA, November 2004.

L. Yang is with the Department of Electrical and Computer Engineering, University of Florida, Gainesville, FL 32611 USA (e-mail: lqyang@ece.ufl.edu).

G. B. Giannakis is with the Department of Electrical and Computer Engineering, University of Minnesota, Minneapolis, MN 55455 USA (e-mail: georgios@ece.umn.edu).

Digital Object Identifier 10.1109/TCOMM.2006.881369

[18]. More recently, baseband real single- and multicarrier (MC) UWB-MA codes have emerged to also avoid narrowband interference (NBI) at low complexity [19].

Parallel with IR-based UWB systems, interest has been growing in multiband (MB) UWB radios. Compared with the aforementioned carrier-free single-band (SB) systems, analog carrier-modulated MB-UWB transmissions may be more sensitive to carrier frequency offsets (CFO), but can easily fit and fill the FCC spectrum mask and thereby avoid NBI by flexible subband selection. The desire for higher data rates and short time-to-market development has further motivated orthogonal frequency-division multiplexing (OFDM)-based MB-UWB, as described in the IEEE 802.15.3a proposals for wireless personal area networks (WPANs) with multiple piconets [1], [3]–[5], [20]. These proposed systems use frequency-hopping (FH) over multiple subbands to support multiple users, and rely on error-control coding (ECC) and interleaving to combat fading and collect the ample multipath diversity provided by UWB links. Even if spectral efficiency is compromised (especially with low-rate ECC), existing MB-UWB schemes do not fully suppress multiuser interference (MUI). On the other hand, in the context of non-UWB wireless communications, OFDM-based MA has been studied extensively. State-of-the-art orthogonal frequency-division MA (OFDMA) in the non-UWB regime include the generalized MC (GMC) code-division MA (CDMA) system, which provides MUI resilience and enables full multipath diversity based on linear complex field (LCF) codes, and the unitary-precoded (UP) OFDMA system which further improves the power and bandwidth efficiency of GMC-CDMA [13], [14], [16].

In this paper, we introduce a crossband flexible UWB (FLEX-UWB) MA scheme for multipiconet WPANs. The FLEX-UWB scheme provides MUI resilience and can be configured as a CDMA, FDMA, or time-division (TD)MA system. Different from the MUI-resilient system introduced in [18], our design here is tailored for an MB system, jointly taking into account all subbands. We derive a unifying fast Fourier transform (FFT)-based MB-UWB system model, and show how existing FH-OFDM proposals fit within this framework. For the OFDM-based access schemes, we adopt LCF encoding to enable multipath diversity without sacrificing bandwidth or complexity. In addition, we also introduce TDMA and CDMA variants of our FLEX-UWB, which can further reduce the system complexity and enhance the rate scalability.

The rest of this paper is organized as follows. In Section II, a unifying FFT-based MB-UWB framework is derived. It is then shown to fit existing FH-OFDM proposals in Section III. Relying on carefully designed user-specific (de)coding and

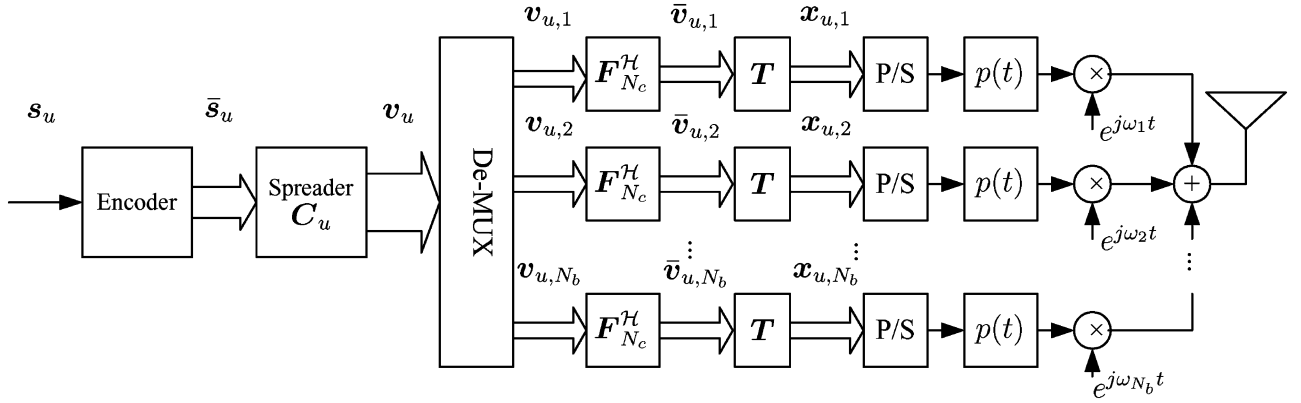


Fig. 1. Block diagram of FFT-based MB-UWB transmitter.

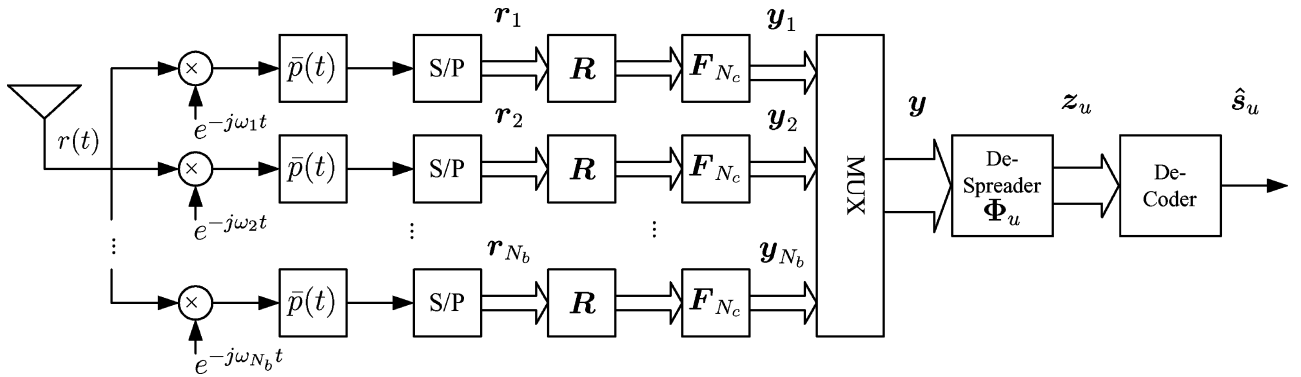


Fig. 2. Block diagram of FFT-based MB-UWB receiver.

(de)spreading matrices, we will derive our FLEX-UWB MA scheme in Section IV. In addition to OFDM-based access schemes, TDMA and CDMA variants will be investigated in Section V. In Section VI, simulated comparisons between FLEX-UWB and existing FH-OFDM radios will be performed for various rates and UWB channels used in the IEEE standard. Summarizing remarks will conclude the paper.

Notation: We will use boldface lower- and upper-case letters \mathbf{a} and \mathbf{A} to represent column vectors and matrices, respectively; \mathbf{I}_N will denote the $N \times N$ identity matrix, and \mathbf{F}_N the $N \times N$ FFT matrix; \mathbf{A}^H will represent the Hermitian of matrix \mathbf{A} ; $\mathbf{e}_N[n]$ and $\mathbf{f}_N[n]$ will stand for the n th column of the $N \times N$ identity and FFT matrices, respectively. $\mathbf{A} \otimes \mathbf{B}$ is the Kronecker product of \mathbf{A} and \mathbf{B} , and δ_n denotes the Kronecker delta function; i.e., $\delta_n = 1$ for $n = 0$, and 0, elsewhere.

II. A GENERAL FFT-BASED MB-UWB SYSTEM MODEL

A generic FFT-based MB-UWB transmitter is depicted in Fig. 1. The total number of subbands is N_b and the number of subcarriers per subband is N_c . We will deal with block-by-block transmissions, where the k th information-bearing block of user u is denoted as $\mathbf{s}_u(k)$. Each such block is first processed by an encoder implementing either a Galois Field (GF) code or a LCF code to enable the channel's multipath diversity. The output of the encoder $\bar{\mathbf{s}}_u(k)$ is then processed by a user-specific $N_b N_c \times N_c$ spreading matrix $\mathbf{C}_u(k)$ to yield the block

$\mathbf{v}_u(k) = \mathbf{C}_u(k)\bar{\mathbf{s}}_u(k)$. The encoder and spreader play key roles in our FLEX-UWB design: they determine the MA scheme, enable multipath diversity, and allow for flexible performance complexity tradeoffs.

The encoded block $\mathbf{v}_u(k)$ is further demultiplexed (De-MUX) into N_b subblocks $\{\mathbf{v}_{u,b}(k)\}_{b=1}^{N_b}$, each of size N_c . These are inverse (I)FFT processed using the $N_c \times N_c$ matrix $\mathbf{F}_{N_c}^H$ before entering the per-subband processor represented by the $N \times N_c$ transmit matrix \mathbf{T} . Being tall ($N \geq N_c$), the latter introduces redundancy in the form of a cyclic prefix (CP) or trailing zeros to avoid interblock interference (IBI), as we detail later. The resultant $N \times 1$ subblock on the b th branch can be written as $\mathbf{x}_{u,b}(k) = \mathbf{T}\mathbf{F}_{N_c}^H \mathbf{v}_{u,b}(k)$. Stacking subblocks $\{\mathbf{x}_{u,b}(k)\}_{b=1}^{N_b}$, we can represent the u th user's digital transmitted block as $\mathbf{x}_u(k) = (\mathbf{I}_{N_b} \otimes \mathbf{T}\mathbf{F}_{N_c}^H)\mathbf{v}_u(k)$. After parallel-to-serial (P/S) conversion, every substream $\mathbf{x}_{u,b}(k)$ is spectrum shaped by $p(t)$ with duration T_p in the nanosecond scale, and modulated by a different analog carrier ω_b , $b = 1, 2, \dots, N_b$. To avoid interference between adjacent subbands, the spacing between adjacent carriers must be no less than $B_p \approx 1/T_p$. If we transmit one symbol per subband with symbol duration T_p , then a total of N_b symbols can be transmitted simultaneously. For an SB-UWB system (a.k.a. impulse radio) to achieve the same rate, each symbol has to be transmitted every T_p/N_b seconds, which entails analog-to-digital/digital-to-analog (AD/DA) converters operating at N_b times higher rate.

The receiver corresponding to this FFT-based MB-UWB transmitter is depicted in Fig. 2. The received signal $r(t)$ is the aggregate of all (N_u) users' signals. On each branch, $r(t)$ is carrier-demodulated by the frequency of the corresponding subband. Sampling the output of the front-end filter matched to $p(t)$, denoted as $\bar{p}(t)$, yields the digital signal per subband. Hence, the received sub-block on the b th branch (subband) becomes $\forall b \in [1, N_b]$: $\mathbf{r}_b(k) = \sum_{u=1}^{N_u} \mathbf{H}_{u,b}^{(0)} \mathbf{T} \bar{\mathbf{v}}_{u,b}(k) + \mathbf{H}_{u,b}^{(1)} \mathbf{T} \bar{\mathbf{v}}_{u,b}(k-1) + \boldsymbol{\eta}_b(k)$, where $\bar{\mathbf{v}}_{u,b}(k) := \mathbf{F}_{N_c}^H \mathbf{v}_{u,b}(k)$, $\boldsymbol{\eta}_b(k)$ is the vector of additive white Gaussian noise (AWGN) samples, $\mathbf{H}_{u,b}^{(0)}$ and $\mathbf{H}_{u,b}^{(1)}$ are $N \times N$ lower- and upper-triangular Toeplitz matrices, with first column $[h_{u,b}(0), \dots, h_{u,b}(L_{u,b}), 0, \dots, 0]^T$ and first row $[0, \dots, 0, h_{u,b}(L_{u,b}), \dots, h_{u,b}(1)]$, respectively, and $L_{u,b}$ is the order of the discrete-time-equivalent channel of the u th user's channel on the b th subband. Notice that by choosing $N > L_{u,b}$, intersymbol interference (ISI) and IBI are confined within two transmitted blocks, and there is no coupling among subbands due to the analog carrier (de)modulation.

Let $N = N_c + L$ with $L := \max_{u,b} \{L_{u,b}\}$ and choose $\mathbf{T} = \mathbf{T}_{N_c, L} := [\mathbf{I}_{N_c}, \mathbf{0}_{N_c \times L}]^T$ to be an $N \times N_c$ zero-padding (ZP) matrix which inserts L trailing zeros to $\bar{\mathbf{v}}_{u,b}(k)$ by premultiplication. It can be easily verified that choosing \mathbf{T} as a ZP matrix ensures $\mathbf{H}_{u,b}^{(1)} \mathbf{T} = \mathbf{0}_{N \times N_c}$ [13, pp. 31–32]. Defining the $N \times N_c$ tall Toeplitz matrix $\mathbf{H}_{u,b} := \mathbf{H}_{u,b}^{(0)} \mathbf{T}$, we can write the IBI-free received subblock as $\mathbf{r}_b(k) = \sum_{u=1}^{N_u} \mathbf{H}_{u,b} \bar{\mathbf{v}}_{u,b}(k) + \boldsymbol{\eta}_b(k)$. By stacking $\{\mathbf{r}_b(k)\}_{b=1}^{N_b}$, we obtain the k th digital received block as

$$\mathbf{r}(k) = \sum_{u=1}^{N_u} \mathbf{H}_u \bar{\mathbf{v}}_u(k) + \boldsymbol{\eta}(k) \quad (1)$$

where $\bar{\mathbf{v}}_u(k) = (\mathbf{I}_{N_b} \otimes \mathbf{F}_{N_c}^H) \mathbf{v}_u(k) = (\mathbf{I}_{N_b} \otimes \mathbf{F}_{N_c}^H) \mathbf{C}_u(k) \bar{\mathbf{s}}_u(k)$ and $\mathbf{H}_u := \text{diag}\{\mathbf{H}_{u,1}, \dots, \mathbf{H}_{u,N_b}\}$ is the block-diagonal channel matrix of the u th user, with each block being an $N \times N_c$ Toeplitz matrix. Note that the vector $\bar{\mathbf{v}}_u(k)$ contains the time-domain data sequence transmitted through the equivalent channel matrix \mathbf{H}_u .

The subblocks $\{\mathbf{r}_b(k)\}_{b=1}^{N_b}$ are then processed by a receive matrix \mathbf{R} followed by the FFT matrix \mathbf{F}_{N_c} . Corresponding to the ZP matrix $\mathbf{T}_{N_c, L}$ at the transmitter, we choose \mathbf{R} to be the ZP-wrapping matrix $\mathbf{R}_{N_c, L} := [\mathbf{I}_{N_c} \mathbf{T}_{N_c, L}^{-1}]$. The resultant subblocks on the b th branch, $\mathbf{y}_b(k) = \mathbf{F}_{N_c} \mathbf{R} \mathbf{r}_b(k)$, are then multiplexed (MUX) to form $\mathbf{y}(k) := [\mathbf{y}_1^T(k), \dots, \mathbf{y}_{N_b}^T(k)]^T = \sum_{u=1}^{N_u} (\mathbf{I}_{N_b} \otimes \mathbf{F}_{N_c} \mathbf{R}) \mathbf{H}_u (\mathbf{I}_{N_b} \otimes \mathbf{F}_{N_c}^H) \mathbf{v}_u(k) + \boldsymbol{\zeta}(k)$, where $\boldsymbol{\zeta}(k)$ is the processed noise vector. Using properties of the Kronecker product and recalling that \mathbf{H}_u is a block-diagonal matrix, the product $(\mathbf{I}_{N_b} \otimes \mathbf{F}_{N_c} \mathbf{R}) \mathbf{H}_u (\mathbf{I}_{N_b} \otimes \mathbf{F}_{N_c}^H)$ is also a block-diagonal matrix. With $\mathbf{T} = \mathbf{T}_{N_c, L}$ and $\mathbf{R} = \mathbf{R}_{N_c, L}$, it can be shown that $\tilde{\mathbf{H}}_{u,b} := \mathbf{R} \mathbf{H}_{u,b} = \mathbf{R} \mathbf{H}_{u,b}^{(0)} \mathbf{T}$ is an $N_c \times N_c$ circulant matrix [13, pp. 31–32].¹ Moreover, pre- and post-multiplying $\tilde{\mathbf{H}}_{u,b}$ with $\mathbf{F}_{N_c}^H$ and \mathbf{F}_{N_c} results in a diagonal matrix $\mathbf{D}_{u,b}$ whose diagonal elements are the subchannel frequency-response samples of the u th user on the FFT grid; that is, $\mathbf{D}_{u,b} = \sqrt{N_c} \text{diag}\{\mathbf{F}_{1:L_{u,b}+1}[h_{u,b}(0), \dots, h_{u,b}(L_{u,b})]^T\}$,

¹This circulant channel matrix we obtained via ZP, can also be obtained by inserting (removing) a CP at the transmitter (receiver).

where $\mathbf{F}_{1:L}$ denotes the $N_c \times L$ matrix consisting of the first L columns of the FFT matrix \mathbf{F}_{N_c} . As a result, the input–output (I/O) relationship of the FFT-based MB-UWB system can be further simplified to

$$\mathbf{y}(k) = \sum_{u=1}^{N_u} \mathbf{D}_u \mathbf{v}_u(k) + \boldsymbol{\zeta}(k) \quad (2)$$

where $\mathbf{D}_u := \text{diag}\{\mathbf{D}_{u,1}, \mathbf{D}_{u,2}, \dots, \mathbf{D}_{u,N_b}\}$.

In the generic system described by (2), each of the N_u users (say the μ th) can theoretically transmit $N_b N_c$ symbols (size of $\mathbf{v}_\mu(k)$) on all the $N_b N_c$ system subcarriers. But due to MUI, this is impossible unless $N_u = 1$. To cope with MUI when $N_u \geq N_b$, each user will transmit at most N_c symbols on N_c subcarriers. User separation will be accomplished by processing $\mathbf{y}(k)$ with a user-specific despreading matrix $\Phi_\mu(k)$ to suppress (or eliminate) MUI and extract the desired user's detection statistic $\mathbf{z}_\mu(k) = \Phi_\mu(k) \mathbf{y}(k)$. The latter can then be processed by the GF or LCF decoder to obtain an estimate of the transmitted block as $\hat{\mathbf{s}}_\mu(k)$. The first approach to separating users in (2) is through FH, as we describe next.

III. FH-OFDM BASED MB-UWB RADIOS IN THE IEEE 803.15.3a PROPOSAL

In this section, we will see how the OFDM-based MB-UWB proposal in the IEEE 802.15.3a standard fits in the general framework of the previous section. In this proposal, the encoder consists of a GF encoder implementing a convolutional code (CC). The CC rate (always < 1) is variable, depending on the required data rate. Each user (piconet) uses OFDM to transmit N_c coded symbols per block $\bar{\mathbf{s}}_u(k)$ on the N_c subcarriers of a single subband. Furthermore, each user relies on a user-specific FH spreading code to hop randomly from subband to subband, one block after the other, thereby effecting what is referred to as time-frequency interleaving (TFI). Relative to (2), MUI in this MB-UWB scheme can be mitigated, but can not be *eliminated*, since users can “collide” on a subband.

To analytically describe this FH-OFDM MB-UWB scheme, let $b_u(k)$ denote the subband index of the k th transmitted block, drawn randomly by user u from the interval $[1, N_b]$. (This is the FH code determining the subband index that user u will use for transmitting his/her k th block.) Since the $N_c \times 1$ block $\bar{\mathbf{s}}_u(k)$ now carries N_c symbols for each k , we can describe this subband selection using the special $N_c N_b \times N_c$ spreading matrix

$$\mathbf{C}_u(k) = \mathbf{e}_{N_b}[b_u(k)] \otimes \mathbf{I}_{N_c} \quad (3)$$

where the column $\mathbf{e}_{N_b}[b_u(k)]$ of the $N_b \times N_b$ identity matrix renders only the $b_u(k)$ th $N_c \times N_c$ submatrix of $\mathbf{C}_u(k)$ nonzero during the k th block. Going back to Fig. 1, recall that $\mathbf{v}_u(k) = \mathbf{C}_u(k) \bar{\mathbf{s}}_u(k)$, and consider how the I/O in (2) changes for this spreading matrix. With $\mathbf{C}_u(k)$ as in (3), the $N_b N_c \times N_c$ matrix $\mathbf{D}_u \mathbf{C}_u(k)$, which consists of N_b vertically stacked $N_c \times N_c$ submatrices, has only its $b_u(k)$ th submatrix $\mathbf{D}_{u,b_u(k)}$ being nonzero. For example, if the u th user's FH code is $b_u(k) = 2$ during the k th block, then $\mathbf{e}_{N_b}[b_u(k)]$ picks up the second column of the $N_b \times N_b$ identity matrix. Consequently, the u th user's symbols are conveyed by the second branch (subband) of

TABLE I
TFI CODES

User u	$b_u(6k)$	$b_u(6k+1)$	$b_u(6k+2)$	$b_u(6k+3)$	$b_u(6k+4)$	$b_u(6k+5)$
1	1	2	3	1	2	3
2	1	3	2	1	3	2
3	1	1	2	2	3	3
4	1	1	3	3	2	2

Fig. 1, which corresponds to the channel response $\mathbf{D}_{u,2}$. The latter then constitutes the only nonzero block of the product $\mathbf{D}_u \mathbf{C}_u(k)$.

At the receiver side, FH-OFDMA relies on the despreading matrix $\mathbf{\Phi}_u(k) = \mathbf{C}_u^H(k)$ to form the detection statistic $\mathbf{z}_\mu(k) = \mathbf{\Phi}_\mu(k) \mathbf{y}(k) = \sum_{u=1}^{N_u} \mathbf{C}_\mu^H(k) \mathbf{D}_u \mathbf{C}_u(k) \mathbf{s}_u(k) + \xi_\mu(k)$. Based on the structure of $\mathbf{D}_u \mathbf{C}_u(k)$ and using properties of Kronecker products, it is easy to verify that $\mathbf{C}_\mu^H(k) \mathbf{D}_u \mathbf{C}_u(k) = \mathbf{e}_{N_b}^T [b_\mu(k)] \mathbf{e}_{N_b} [b_u(k)] \mathbf{D}_{u,b_u(k)} = \delta_{b_\mu(k)-b_u(k)} \mathbf{D}_{u,b_u(k)}$. This simplifies the μ th user's decision statistic to

$$\mathbf{z}_\mu(k) = \mathbf{D}_{\mu,b_\mu(k)} \mathbf{s}_\mu(k) + \sum_{u \neq \mu} \delta_{b_\mu(k)-b_u(k)} \mathbf{D}_{u,b_u(k)} \mathbf{s}_u(k) + \xi_\mu(k)$$

where the MUI represented by the last sum is nonzero whenever $b_\mu(k) = b_u(k) \forall u \neq \mu$. Certainly, if we have, at most, as many users as subbands ($N_u \leq N_b$), then we can have FH codes ensuring collision-free MA. But even in such cases, MUI elimination requires all users' FH codes to be synchronized, since asynchronism can result in catastrophic collisions. To avoid this problem, special FH (a.k.a. TFI) codes are proposed in the IEEE802.15.3a standard, where typical system parameters are $N_c = 128$, $N_b = 3$, and $N_u = 4$, as shown in Table I [4]. Such FH codes can be deployed in an asynchronous manner without inducing catastrophic collisions. However, at least two users transmit over the same subband during any block (see Table I); and for this reason, MUI is inevitable.

The FH-OFDM based MB-UWB scheme only requires a single oscillator that changes oscillating frequency from block to block. Moreover, with each user occupying a single subband all the time, the raw data rate (transmission rate) is fixed to N_c symbols per block per user, regardless of the number of users N_u . However, these benefits do not come for free: 1) FH among multiple bands with a single oscillator entails very short switching and stabilization time, which may increase the severity of CFOs; 2) to capitalize on the ample multipath diversity provided by the UWB channel, existing FH-OFDM systems rely on GF-based ECC. Together with FH and interleaving, ECC enables diversity collection at the price of reduced spectral efficiency and increased complexity; and 3) TFI codes as in Table I do not eliminate MUI, which degrades error performance and, in turn, reduces the effective information data rate. In the ensuing section, we will see how the FH-OFDM scheme can be improved by allocating subcarriers to different users across subbands.

IV. OFDM-BASED FLEX-UWB

The goal in the novel MA scheme of this section is to deterministically eliminate MUI and effect multipath diversity even

for uncoded OFDM-based MB-UWB transmissions by judiciously designing the outer codec and the inner (de)spreading matrix $(\mathbf{\Phi}_u) \mathbf{C}_u$.

As discussed in the preceding section, GF-based ECC enables multipath diversity at the price of reduced spectral efficiency. On the other hand, LCF encoders have been designed to enable space and multipath diversity, as well as improve power and bandwidth efficiency in conventional single- and multiantenna systems; see, e.g., [9], [16], and [17]. In our FLEX-UWB, the GF-based ECC module will be replaced by an LCF encoding matrix $\mathbf{\Theta}_u(k)$. This replacement will considerably improve the effective data rate, even with the spreading matrix $\mathbf{C}_u(k)$ in (3).

The LCF encoder chosen is the $N_c \times N_c$ matrix $\mathbf{\Theta}_u(k) = \mathbf{F}_{N_c}^H \text{diag}\{1, \alpha, \dots, \alpha^{N_c-1}\}$, where $\alpha = e^{j\pi/(2N_c)}$, and is applied to each user's $N_c \times 1$ symbol vector $\mathbf{s}_u(k)$ to yield $\bar{\mathbf{s}}_u(k) = \mathbf{\Theta}_u(k) \mathbf{s}_u(k)$. Notice that since $\mathbf{\Theta}_u(k)$ is square, no redundancy is added, and $\mathbf{\Theta}_u(k)$ remains the same $\forall k, u$, because α only relies on N_c . It has been shown that such a $\mathbf{\Theta}_u(k)$ encoder enables the maximum diversity order $L_{u,b_u(k)} + 1$ that the intended channel can provide, so long as $N_c > L_{u,b_u(k)}$ (see, e.g., [9], [16], and [17]).

The LCF encoding matrix $\mathbf{\Theta}_u(k)$ effects multipath diversity without introducing redundancy. However, as mentioned in the preceding section, MUI-resilient spreading with the matrix $\mathbf{C}_u(k)$ in (3) requires synchronous deployment of FH sequences at all piconets, while the asynchronous TFI sequences in Table I can not eliminate MUI. On the other hand, since $\mathbf{\Theta}_u(k)$ enables multipath diversity in any single block k , our new scheme based on LCF encoding does not need FH/TFI. Hence, our FLEX scheme further allows adjusting the number of subcarriers per user (piconet) depending on the number of active users N_u . Different from the FH approach with $\mathbf{C}_u(k)$ as in (3), where each user always transmits N_c symbols per block on N_c subcarriers regardless of the number of active users, each FLEX user transmits $M_u := N_c N_b / N_u$ symbols per block on M_u subcarriers (out of the total $N_c N_b$ system subcarriers). More specifically, when $N_u < N_b$, FLEX allows $M_u > N_c$ to increase the data rate. When $N_u > N_b$, each FLEX user sends $M_u < N_c$ symbols per block. Though the latter appears to lower the *transmission rate*, by allowing each user (piconet) to transmit on distinct subcarriers, it ensures MUI-resilient communication, and can end up with higher effective *information rate*. A second key difference is that the M_u subcarriers of each FLEX user are equally (and maximally) spaced across all N_b subbands, in contrast to FH, where each user's N_c subcarriers are from a single subband in any given block k . This spacing allows FLEX to enhance the achievable multipath diversity in any single block k without invoking ECC and/or TFI.

Even though the aforementioned subcarrier allocation can be adapted to each user's possibly variable load requirement, we will suppose for simplicity that the allocation is invariant across blocks, and for this reason, we will drop the index k . Next, we will describe the FLEX designs in terms of the LCF encoder Θ_u and the (de)spreading matrix $(\Phi_u)\mathbf{C}_u$. Upon defining $P := M_u/N_b = N_c/N_u$, the matrix determining subcarrier spacing across subbands can be written as $\mathbf{C}_u := \mathbf{I}_{N_b} \otimes (\mathbf{c}_u \otimes \mathbf{I}_P)$ with spreading vector $\mathbf{c}_u = \mathbf{e}_{N_u}[u]$. The latter implies that, e.g., user 1 transmits with subcarriers 1, 2, \dots , P on each of the N_b subbands; and generally, user u transmits with subcarriers $\{uP - p\}_{p=0}^{P-1}$ on each subband.

A so-designed spreading matrix \mathbf{C}_u , together with $\Phi_u = \mathbf{C}_u^H$, enable MUI-resilient access, regardless of the channel and encoding matrix Θ_u . This can be shown from the μ th user's decision statistic

$$\begin{aligned} z_\mu &= \Phi_\mu \mathbf{y} \\ &= \sum_{u=1}^{N_u} \Phi_\mu \mathbf{D}_u \Theta_u \mathbf{s}_u + \xi_\mu = \sum_{u=1}^{N_u} \mathbf{C}_\mu^H \mathbf{D}_u \mathbf{C}_u \Theta_u \mathbf{s}_u + \xi_\mu \end{aligned} \quad (4)$$

where $\mathbf{C}_\mu^H \mathbf{D}_u \mathbf{C}_u$ is a block-diagonal matrix, with diagonal blocks given by $(\mathbf{c}_\mu \otimes \mathbf{I}_P)^H \mathbf{D}_{u,b} (\mathbf{c}_\mu \otimes \mathbf{I}_P) \forall b \in [1, N_b]$. The latter can be further shown to be $\delta_{\mu-u} \mathbf{D}_{u,b} (\mathbf{c}_u \otimes \mathbf{I}_P)$, when $\mathbf{c}_u = \mathbf{e}_{N_u}[u]$. Consequently, we have

$$z_\mu = \Phi_\mu \mathbf{y} = \mathbf{D}_\mu \mathbf{C}_\mu \Theta_\mu \mathbf{s}_\mu + \xi_\mu \quad (5)$$

which is deterministically free of MUI. Intuitively speaking, with $\mathbf{c}_u = \mathbf{e}_{N_u}[u]$, matrix \mathbf{C}_u assigns distinct subcarriers to individual users, and \mathbf{C}_u^H extracts these distinct subcarriers at the receiver and eliminates MUI, regardless of the channel and encoding matrix Θ_u . Further, by construction of \mathbf{C}_u , the subcarriers allocated to each user are not from a single subband, but from all subbands. On each of the N_b subbands, the u th user occupies the $(uP - P + 1)$ st through the uP th subcarriers and transmits one symbol over each of them. In other words, $\mathbf{c}_u = \mathbf{e}_{N_u}[u]$ gives rise to a crossband OFDMA scheme.

However, it is well known that OFDM can only provide diversity order 1, regardless of the UWB multipath channel. This is clear from the diagonal channel structure $\mathbf{D}_\mu \mathbf{C}_\mu$ in (5). The problem is amended by the $M_u \times M_u$ LCF encoding matrix $\Theta_u = \mathbf{F}_{M_u}^H \text{diag}\{1, \alpha, \dots, \alpha^{M_u-1}\}$, with $\alpha = e^{j\pi/(2M_u)}$. In an MB-UWB setup, our crossband design can be summarized as follows.

Proposition 1: The user-specific encoding and (de)spreading matrices are designed as

$$\begin{aligned} \Theta_u &= \mathbf{F}_{M_u}^H \text{diag}\{1, \alpha, \dots, \alpha^{M_u-1}\}, \\ \mathbf{C}_u &= \mathbf{I}_{N_b} \otimes (\mathbf{e}_{N_u}[u] \otimes \mathbf{I}_P) \quad \text{and} \\ \Phi_u &= \mathbf{I}_{N_b} \otimes (\mathbf{e}_{N_u}[u] \otimes \mathbf{I}_P)^H \end{aligned} \quad (6)$$

where $\alpha = e^{j\pi/(2M_u)}$. They ensure MUI-resilient UWB access without sacrificing bandwidth efficiency, and enable diversity order $\sum_{b=1}^{N_b} \min\{M_u/N_b, L_{u,b} + 1\} \leq \min\{M_u, \sum_{b=1}^{N_b} (L_{u,b} + 1)\}$, where $L_{u,b}$ is the u th user's subchannel order on the b th subband. In addition, when $M_u/N_b \geq L_{u,b} \forall b = 1, 2, \dots, N_b$, the maximum diversity order $\sum_{b=1}^{N_b} (L_{u,b} + 1)$ is achieved.

Proof: See Appendix I. ■

Proposition 1 asserts that with crossband subcarrier allocation, it is possible to collect the multipath diversity from all N_b subbands. In fact, along the lines of the proof of *Proposition 1*, it can be readily shown that subcarrier assignment within a single (say, the b th) subband can only enable diversity of order equal to $\min\{M_u, L_{u,b} + 1\}$, which is upper bounded by $(L_{u,b} + 1)$ as opposed to $\sum_{b=1}^{N_b} (L_{u,b} + 1)$ in *Proposition 1*.

To collect the diversity gain enabled by the encoder, the decoder can be either a sphere decoder (SD) that yields exact or near maximum-likelihood (ML) performance at polynomial complexity, or reduced-complexity alternatives such as block zero-forcing (ZF) or minimum mean-square error (MMSE) decision-feedback equalizers [2], or even linear decoders, including ZF and MMSE ones. Since MUI is removed deterministically, each piconet can choose its decoder based on the bit-error rate (BER) and complexity requirements set by its own service. As usual, there is a tradeoff between decoding complexity and error performance: to fully collect the diversity enabled by the LCF encoder, exact or near ML decoders have to be used. From *Proposition 1*, it is also clear that the achievable diversity order heavily depends on the size of the LCF coder; while the latter directly affects the decoding complexity.

A. Reduced-Complexity Demodulation With Grouping

When the encoder size M_u is large, the decoding complexity can be prohibitively high. On the other hand, one generally needs to collect *sufficiently high* multipath diversity, as opposed to *full* multipath diversity, especially in UWB channels. Trading performance for reduced complexity, each block of symbols can be divided into groups, and LCF can be applied on each group of smaller size as in [8]. In our MB-UWB context, we divide each user's $M_u \times 1$ transmitted symbol block \mathbf{s}_u into crossband groups, each of which contains N_g symbols. Following the arguments in [8] and, a carefully designed $N_g \times N_g$ LCF encoder will enable diversity order N_g .

Proposition 2: Let $\mathbf{c}_u = \mathbf{e}_{N_u}[u]$, and

$$\Theta_u = \left(\mathbf{F}_{N_g}^H \text{diag}\{1, \alpha, \dots, \alpha^{N_g-1}\} \right) \otimes \mathbf{I}_{M_u/N_g} \quad (7)$$

where $N_g (\ll L, M_u)$ is the group size and $\alpha = e^{j\pi/(2N_g)}$. Then the user-specific (de)spreading matrices $\mathbf{C}_u = \mathbf{I}_{N_b} \otimes (\mathbf{c}_u \otimes \mathbf{I}_P)$ and $\Phi_u = \mathbf{C}_u^H$, together with Θ_u , ensure MUI-resilient UWB-MA without sacrificing bandwidth efficiency, while enabling diversity order N_g .

Notice that our encoder Θ_u consists of two parts: $\mathbf{F}_{N_g}^H \text{diag}\{1, \alpha, \dots, \alpha^{N_g-1}\}$ performs LCF coding within groups of size N_g ; and $\otimes \mathbf{I}_{M_u/N_g}$ implements the grouping operation. By the definition of Kronecker products, it can be easily deduced that the N_g symbols of each group are maximally and equally spaced in the $M_u \times 1$ symbol blocks of each user. Our simulations will corroborate that such an interleaved grouping strategy provides performance advantage over the uninterleaved grouping strategy.

So far, we have exposed the OFDM-based FLEX-UWB scheme with LCF encoding, which can be coupled with either FH/TFI or with crossband subcarrier allocation. While the

latter deterministically mitigates MUI, it entails N_b local oscillators. However, since FH is not needed, these oscillators can have relatively longer stabilization period to alleviate possible CFO effects. In addition, the crossband subcarrier allocation, together with LCF encoding, enable full multipath diversity without bandwidth expansion. Reduced-complexity demodulation is also possible by trading off performance for complexity through crossband subcarrier grouping.

V. FLEXIBLE MULTIACCESS

Our framework also extends to non-OFDM-based MA schemes through different choices of \mathbf{c}_u , the OFDM one corresponding to $\mathbf{c}_u = \mathbf{e}_{N_u}$. We will see that with linear receivers, generalized FLEX-UWB schemes can achieve BER performance that is comparable to the LCF-encoded OFDM-based FLEX-UWB scheme, and better than the convolutionally coded FH-OFDM scheme. They will also turn out to be more flexible in providing variable data rates.

With the OFDM-based FLEX-UWB system, MUI mitigation relies on the fact that

$$\mathbf{C}_\mu^H \mathbf{D}_u \mathbf{C}_u = \mathbf{D}_\mu \mathbf{C}_\mu \delta_{u-\mu} \quad (8)$$

when $\mathbf{c}_u = \mathbf{e}_{N_u}[u]$ [c.f. (4)]. However, for general code vectors $\{\mathbf{c}_u\}_{u=1}^{N_u}$ that are mutually orthogonal with unit norm $\mathbf{c}_u^H \mathbf{c}_\mu = \delta_{u-\mu}$, the relationship (8) does not hold, in general. Intuitively speaking, when $\mathbf{c}_u \neq \mathbf{e}_{N_u}[u]$, more than one user shares the same subcarrier(s), and special designs are needed to avoid MUI.

Let us consider now the equivalent spreading matrix \mathbf{A}_u which relates $\bar{\mathbf{s}}_u$ with $\bar{\mathbf{v}}_u = \mathbf{A}_u \bar{\mathbf{s}}_u$ that contains the time-domain data sequence to be transmitted [c.f. (1)]. In the preceding section, we proved that $\mathbf{A}_u = (\mathbf{I}_{N_b} \otimes \mathbf{F}_{N_c}^H) \mathbf{C}_u = \mathbf{I}_{N_b} \otimes \mathbf{F}_{N_c}^H (\mathbf{c}_u \otimes \mathbf{I}_P)$ preserves the mutual orthogonality among users after propagating through unknown multipath channel, when user-specific codes are chosen as $\mathbf{c}_u = \mathbf{e}_{N_u}[u]$. For any orthonormal \mathbf{c}_u , we further establish the following.

Lemma 1: The mutual orthogonality among users can be preserved by $\mathbf{A}_u = \mathbf{I}_{N_b} \otimes [\mathbf{F}_{N_c}^H (\mathbf{c}_u \otimes \mathbf{I}_P) \otimes \mathbf{T}_{K,L}]$ for any orthonormal \mathbf{c}_u , where $\mathbf{T}_{K,L} := [\mathbf{I}_K, \mathbf{0}_{K \times L}]^T$ is the $(K+L) \times K$ ZP matrix, even after propagating through (possibly unknown) multipath channels.

Proof: Letting $\bar{N} := N_b N_c (K+L)$, the I/O relationship between the $\bar{N} \times 1$ transmitted and received vectors is

$$\mathbf{r} = \sum_{u=1}^{N_u} \bar{\mathbf{H}}_u^{(0)} \bar{\mathbf{v}}_u + \boldsymbol{\eta} = \sum_{u=1}^{N_u} \bar{\mathbf{H}}_u^{(0)} \mathbf{A}_u \boldsymbol{\Theta}_u \mathbf{s}_u + \boldsymbol{\eta} \quad (9)$$

where $\bar{\mathbf{H}}_u^{(0)} := \text{diag}\{\bar{\mathbf{H}}_{u,1}^{(0)}, \dots, \bar{\mathbf{H}}_{u,N_b}^{(0)}\}$ is the block-diagonal channel matrix of the u th user, with each block being an $\bar{N} \times \bar{N}$ lower-triangular Toeplitz matrix.

In Appendix II, we prove that

$$\bar{\mathbf{H}}_u^{(0)} \mathbf{A}_u = \mathbf{B}_u \bar{\mathbf{H}}_u \quad (10)$$

where $\mathbf{B}_u := \mathbf{F}_{N_c}^H (\mathbf{c}_u \otimes \mathbf{I}_P) \otimes \mathbf{I}_{K+L}$, $\bar{\mathbf{H}}_u := \text{diag}\{\mathbf{I}_P \otimes \bar{\mathbf{H}}_{u,1}, \dots, \mathbf{I}_P \otimes \bar{\mathbf{H}}_{u,N_b}\}$ and $\bar{\mathbf{H}}_{u,b}$ are $(K+L) \times K$ lower-triangular Toeplitz matrices, with the first column given by

$[h_{u,b}(0), \dots, h_{u,b}(L), 0, \dots, 0]^T$. The mutual orthogonality among users is thereby preserved, since $\mathbf{B}_\mu^H \mathbf{B}_u = \mathbf{I}_{K+L} \delta_{u-\mu}$. ■

From (10), it naturally follows that the μ th user's equivalent despreading processor should be \mathbf{B}_μ^H to yield the decision statistic

$$\begin{aligned} \mathbf{z}_\mu &= \mathbf{B}_\mu^H \mathbf{r} \\ &= [(\mathbf{c}_\mu \otimes \mathbf{I}_P)^H \mathbf{F}_{N_c} \otimes \mathbf{I}_{K+L}] \cdot \mathbf{r} \\ &= \bar{\mathbf{H}}_\mu \boldsymbol{\Theta}_\mu \bar{\mathbf{s}}_\mu + \boldsymbol{\xi}_\mu. \end{aligned} \quad (11)$$

Notice that every diagonal block of $\bar{\mathbf{H}}_u$ is a tall Toeplitz matrix. As long as $\{h_{u,b}(l)\}_{l=0}^L$ are not all zeros, matrix $\bar{\mathbf{H}}_{u,b}$ will have full column rank. In other words, full diversity per subband is guaranteed, even without GF or LCF encoding. Although $\boldsymbol{\Theta}_u$ can be designed to enable diversity collection across subbands, this will significantly increase decoding complexity. In addition, very large diversity gain will only show up at a very high signal-to-noise ratio (SNR). For this reason, we simply let $\boldsymbol{\Theta}_u = \mathbf{I} \forall u$. Mapping the equivalent spreading and despreading matrices \mathbf{A}_u and \mathbf{B}_u back to the (de)spreader \mathbf{C}_u and $\boldsymbol{\Phi}_u$, it turns out that the MA-enabling operator $\mathbf{C}_u = \mathbf{I}_{N_b} \otimes (\mathbf{c}_u \otimes \mathbf{I}_P)$ is still valid, provided that the \mathbf{T} and \mathbf{R} blocks are replaced by interleavers. More specifically, we have the following FLEX design.

Proposition 3: With any set of orthogonal codes $\{\mathbf{c}_u\}_{u=1}^{N_u}$, the user-specific encoding and decoding matrices are designed as

$$\boldsymbol{\Theta}_u = \mathbf{I}, \quad \mathbf{C}_u = \mathbf{I}_{N_b} \otimes (\mathbf{c}_u \otimes \mathbf{I}_P) \quad \text{and} \quad \boldsymbol{\Phi}_u = \mathbf{C}_u^H \quad (12)$$

with the transmitter and receiver diagrams given in Figs. 3 and 4, respectively. They ensure MUI-resilient UWB access and enable diversity order $\min_{b \in [1, N_b]} \{L_{u,b} + 1\}$, where $L_{u,b}$ is the u th user's subchannel order on the b th subband.

Because \mathbf{A}_u already contains L trailing zeros, IBI is absent even without the \mathbf{T} processor after the IFFT. Instead, an interleaver $\boldsymbol{\pi}_1$ replaces the \mathbf{T} block when TDMA/CDMA user codes are deployed, as shown in Fig. 3. The structure of $\boldsymbol{\pi}_1$ in Fig. 3 indicates that, in addition to interleaving the IFFT-transformed symbols, it also introduces L guard zeros between blocks of size K . Correspondingly, the \mathbf{R} block used at the OFDM-based MB receivers is also replaced with an interleaver $\boldsymbol{\pi}_2$, as depicted in Fig. 4. Notice that for various user codes \mathbf{c}_u , only slight modifications are needed on the original FFT-based MB-UWB transceiver structures.

This generalized FLEX-UWB scheme can accommodate any set of orthogonal user codes \mathbf{c}_u and gives rise to different MA schemes. To appreciate this flexibility, let us consider a particular choice of $\mathbf{c}_u = \mathbf{f}_{N_u}[u]$, which is the u th column of the $N_u \times N_u$ FFT matrix. Corresponding to this choice, the encoded block before the interleaver is $\bar{\mathbf{v}}_u = (\mathbf{I}_{N_b} \otimes \mathbf{F}_{N_c}^H (\mathbf{c}_u \otimes \mathbf{I}_P)) \mathbf{s}_u$. It can be readily verified that the (m, p) th entry of the $N_c \times P$ matrix $\mathbf{F}_{N_c}^H (\mathbf{c}_u \otimes \mathbf{I}_P)$ is

$$\begin{aligned} & \left[\mathbf{F}_{N_c}^H (\mathbf{c}_u \otimes \mathbf{I}_P) \right]_{m,p} \\ &= \frac{1}{\sqrt{N_c N_u}} \sum_{k=0}^{N_u-1} e^{-j \frac{2\pi}{N_c} (m-1)(kP+(p-1))} e^{j \frac{2\pi}{N_u} (u-1)k} \\ &= \frac{1}{\sqrt{P}} e^{-j \frac{2\pi}{N_c} (m-1)(p-1)} \delta_{\text{mod}(m-u, N_u)}. \end{aligned} \quad (13)$$

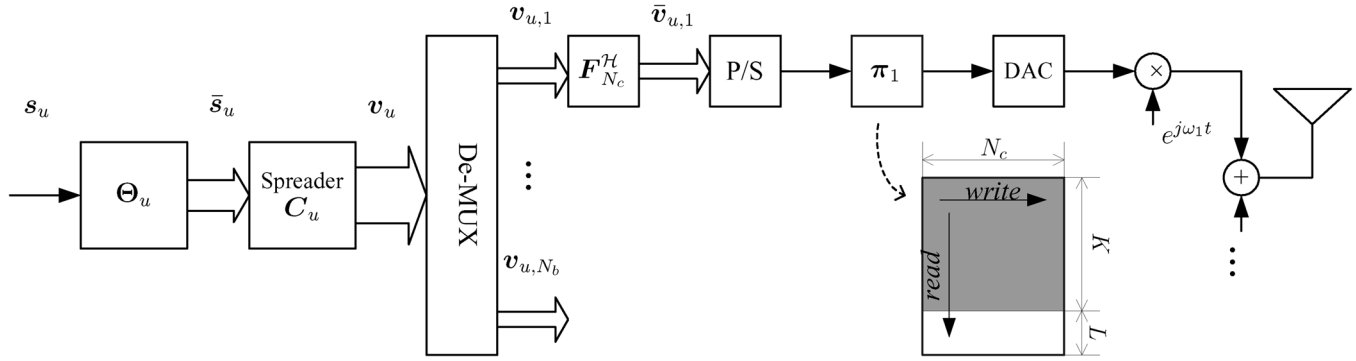


Fig. 3. Block diagram of FLEX-UWB transmitter with TDMA/CDMA user codes.

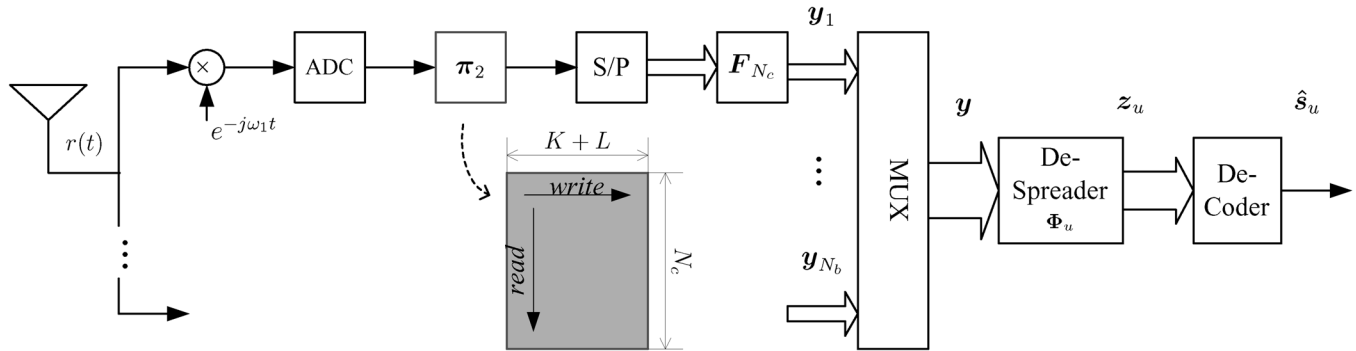


Fig. 4. Block diagram of FLEX-UWB receiver with TDMA/CDMA user codes.

This implies that users take turns in transmitting information symbols using all subcarriers across all subbands; that is, MA is accomplished through time division.

In addition to being flexible in MA schemes, our generalized FLEX-UWB is also flexible in rate scalability. With the encoder being set to $\Theta_u = \mathbf{I}$, the decision statistic simplifies to $\mathbf{z}_u = \bar{\mathbf{H}}_u \mathbf{s}_u + \xi_u$. Further, notice that $\bar{\mathbf{H}}_u$ has a block diagonal structure with each block being a $(K+L) \times K$ Toeplitz matrix. As a result, equalization can be performed on symbols in groups of size K , which is independent of the FFT/IFFT size N_c and the number of users N_u .

Since L guard zeros are inserted following every group of K symbols, the overall bandwidth efficiency is $K/(K+L)$. Clearly, as K increases, bandwidth efficiency also increases but comes also with higher equalization complexity. The OFDM-based FLEX-UWB with $\mathbf{e}_u = \mathbf{e}_{N_c}[u]$, on the other hand, has overall bandwidth efficiency of $N_c/(N_c+L)$, which is fixed given the FFT size N_c and ZP length L . Hence, FLEX-UWB with generic orthonormal user codes \mathbf{e}_u can provide a wider range of data rates. For the TDMA/CDMA-based FLEX-UWB to attain the same data rate as the OFDM-based FLEX-UWB, one needs $K = N_c$. It is also worth mentioning that, unlike OFDM-based FLEX-UWB which collects multipath diversity relying on LCF encoding, TDMA/CDMA-based FLEX-UWB collect multipath diversity even with linear equalizers. Our simulations will reveal that with a linear MMSE equalizer, the latter can achieve the same error performance as the former at identical data rates.

So far, our design has focused on multiple piconets having comparable data flows. When their data-rate requirements are

different, each user's symbol block size M_u can be adjusted, and more than one orthonormal code \mathbf{e}_u can be assigned to piconets with high data flow. By the design of FLEX-UWB, not only the interference among multiple piconets is eliminated, but also the multiple data streams from a single piconet are not interfering. Hence, flexible multirate MA without sacrificing MUI resilience and bandwidth efficiency is possible, as in [18].

VI. SIMULATIONS

In this section, we will compare the simulated performance of FH-OFDM UWB-MA and our FLEX-UWB on an MB-UWB system with $N_b = 3$ subbands and $N_c = 128$ subcarriers per subband. With $T_p = 1.8939$ ns, the bandwidth of each subband is $B_p = 528$ MHz. To eliminate IBI, the number of trailing zeros is $L = 37$. The duration of each OFDM block is then $(N_c + L)T_p = 312.5$ ns. The number of active WPAN piconets (users) is $N_u = 4$. With quaternary phase-shift keying (QPSK) modulation, the raw data rate attained by the FH (TFI) codes in [4] is $2N_c/312.5$ ns = 819.2 Mb/s per user, and that enabled by OFDM-based FLEX-UWB is $(N_b/N_u)819.2 = 614.4$ Mb/s per user. The LCF group size for OFDM-based FLEX-UWB is $N_g = 4$, and $\alpha = \exp(j\pi/8)$ is chosen as suggested in the systematic design of, e.g., [8] and [9]. In all simulations, the 802.15.3a standardized UWB channel model [6] is used.

Although the raw data rate achieved by FH-OFDM is higher than the OFDM-based FLEX-UWB, the effective information data rate of FH-OFDM also depends on the rate of the CCs employed to combat frequency selectivity of the propagation channel. In the ensuing comparisons, the FH-OFDM system uses CCs of rate 3/4, which yield an effective information data

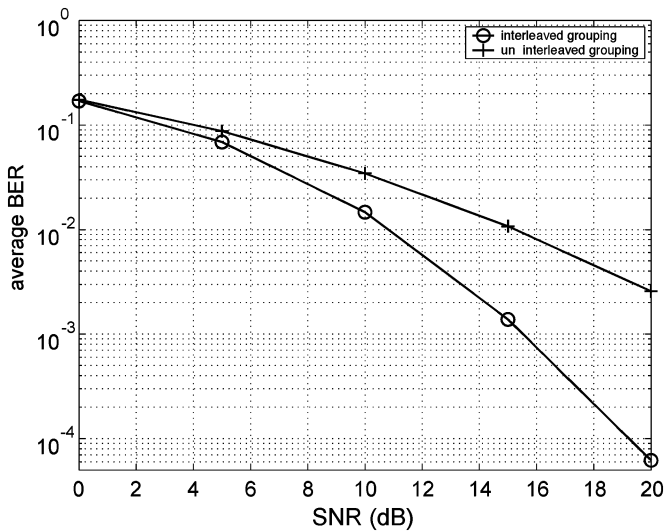


Fig. 5. Average BER versus SNR for IEEE 802.15.3a channel model 1. The interleaved grouping strategy is as in *Proposition 2*.

rate of 614.4 Mb/s. The CC is generated by puncturing the rate-1/3 CC with constraint length 7 and generator polynomials $g_0 = 1338$, $g_1 = 1458$, and $g_2 = 1758$ [4]. To collect multipath diversity, a symbol block interleaver is also employed, followed by a tone interleaver, as in [4].

The effective information rate of the OFDM-based FLEX-UWB system equals the raw data rate 614.4 Mb/s, because the LCF codes do not introduce any redundancy. For the T/CDMA-based FLEX-UWB without any coding, the effective information rate depends on the block size K . For the fairness of the comparison, we choose $K = 128$ to obtain the information rate of 614.4 Mb/s.

Notice that the FLEX-UWB uses all $N_b = 3$ subbands simultaneously, while each user of the FH-OFDM scheme uses one subband at a time. Hence, the FH-OFDM has a $10 \log_{10}(N_b)$ dB power advantage, compared with the FLEX-UWB, subject to the FCC mask. In all figures, the x-axis indicates the SNR of the FLEX-UWB, and the SNR of the FH-OFDM has an additional $10 \log_{10}(N_b)$ dB. However, this power advantage comes at the price of MUI. It is worth reiterating that FLEX-UWB is MUI-resilient by design, while FH-UWB is not. For example, the TFI codes in Table I indicate that the first user in a FH-OFDM system with $N_u = 4$ will inevitably experience interference from both the second and the third user, whereas the interference from the fourth user can be avoided by carefully aligning their FH codes. In our simulations, we supposed that only two interferers are present for FH-UWB, to avoid the worst-case scenario.

First, we compare the average BER performance of the OFDM-based FLEX-UWB with interleaved grouping, as in *Proposition 2* and the uninterleaved grouping. The same group size $N_g = 4$ and the same LCF code are used for both grouping strategies. The plots in Fig. 5 show that the interleaved grouping considerably outperforms the uninterleaved one. The performance advantage at 10^{-3} BER is about 6 dB.

To compare the OFDM-based FLEX-UWB with FH-OFDM systems, the simulated average BER versus SNR is depicted in Fig. 6 for FH-OFDM and our OFDM-based FLEX-UWB.

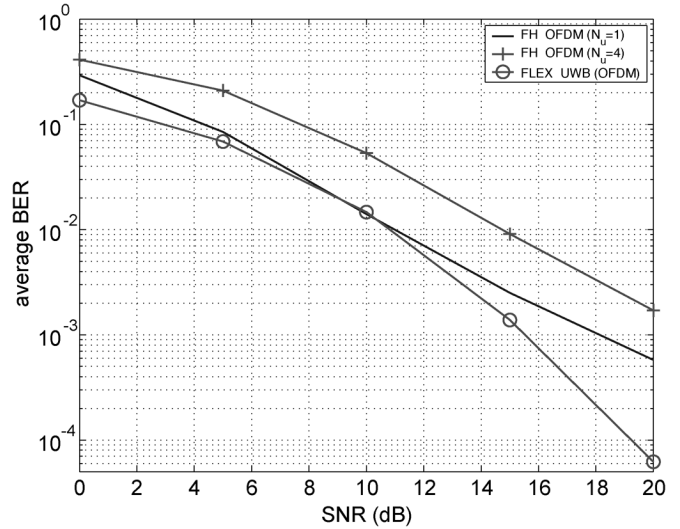


Fig. 6. Average BER versus SNR for IEEE 802.15.3a channel model 1. The data rate is 614.4 Mb/s. Rate-3/4 CC is used for the FH-OFDM. LCF precoding is used for the OFDM-based FLEX-UWB with $N_u = 4$.

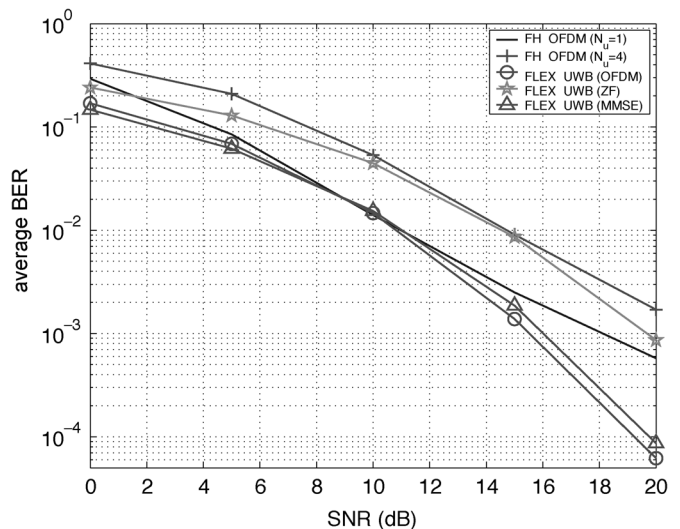


Fig. 7. Average BER versus SNR for IEEE 802.15.3a channel model 1. The data rate is 614.4 Mb/s. Rate-3/4 CC is used for FH-OFDM. The uncoded ZF/MMSE FLEX-UWB systems have $N_u = 4$ active users.

We observe that our OFDM-based FLEX-UWB with four users outperforms the 3/4 convolutionally coded FH-OFDM system, even when MUI is absent. When MUI is present (two interferers each with 0 dB average received SNR), a performance degradation of about 4 dB can be observed for FH-OFDM.

The performance of TDMA/CDMA-based FLEX-UWB is tested and compared with 3/4 convolutionally coded FH-OFDM and OFDM-based FLEX-UWB, as shown in Fig. 7. As expected, the MMSE receiver provides better performance than the ZF receiver for the TDMA/CDMA-based FLEX-UWB. Notice that at identical data rates, the one with MMSE reception exhibits the same BER as the OFDM-based FLEX-UWB system with LCF encoding ($N_g = 4$) and sphere decoding performed at the receiver. In the absence of MUI, the coded FH-OFDM scheme outperforms the uncoded TDMA/CDMA-based FLEX-UWB with a ZF receiver.

However, in the presence of MUI, all FLEX-UWB schemes outperform the coded FH-OFDM scheme. It is worth stressing that the MMSE and ZF options only rely on linear receivers and do not invoke any coding, precoding, or interleaving.

VII. CONCLUSIONS

In this paper, we designed crossband flexible MB-UWB encoding and decoding modules for use in various MA schemes including OFDMA, TDMA, and CDMA. All these MA schemes can be implemented with minor modifications on a core FFT-based MB-UWB transceiver structure. Our designs enable simultaneous access of multiple WPAN piconets without MUI, and can be readily extended to the scenario where the piconets have uneven data flows to allow high-data-flow piconets to transmit multiple decoupled data streams. In addition, the OFDM-based FLEX-UWB relies on crossband application of LCF encoding to collect multipath diversity without bandwidth expansion; while the TDMA/CDMA-based FLEX-UWB enjoys good performance even with linear receivers, and enables tunable data rates.

APPENDIX I

PROOF OF Proposition 1

Applying the standard pairwise error probability (PEP) analysis (see, e.g., [8]), it can be shown that the diversity order is determined by the rank of the following matrix:

$$\Xi_{u,\epsilon} = \mathcal{F}_u^H \mathbf{C}_u \mathcal{D}_\epsilon^H \mathcal{D}_\epsilon \mathbf{C}_u^H \mathcal{F}_u$$

where $\mathcal{F}_u := \text{diag}\{\mathbf{F}_{1:L_{u,1}}, \mathbf{F}_{1:L_{u,2}}, \dots, \mathbf{F}_{1:L_{u,N_b}}\}$ is a block diagonal matrix, with each submatrix being a truncated FFT matrix and $\mathcal{D}_\epsilon := \text{diag}\{\Theta_u \epsilon_u\}$, with $\epsilon_u := \mathbf{s}'_u - \mathbf{s}_u \neq \mathbf{0}$ being the error vector. The u th user's diversity order is

$$G_u = \min_{\forall \epsilon_u \neq \mathbf{0}} \text{rank}\{\Xi_{u,\epsilon}\}.$$

With $\Theta_u = \mathbf{F}_{M_u}^H \text{diag}\{1, \alpha, \dots, \alpha^{M_u-1}\}$, it is ensured that \mathcal{D}_ϵ has full rank, i.e., $\text{rank}\{\mathcal{D}_\epsilon\} = M_u \forall \epsilon \neq \mathbf{0}$. As columns of \mathbf{C}_u are columns of \mathbf{I}_{M_u} and \mathcal{F}_u is blockwise Vandermonde, we deduce that the achievable diversity order for the u th user is

$$G_u = \sum_{b=1}^{N_b} \min \left\{ \frac{M_u}{N_b}, L_{u,b} + 1 \right\}.$$

When $M_u/N_b > L_{u,b} \forall b$, the maximum diversity order $G_{u,\max} = \sum_{b=1}^{N_b} (L_{u,b} + 1)$ is achieved.

APPENDIX II

PROOF OF Lemma 1

By the construction of \mathbf{A}_u , it follows that

$$\bar{\mathbf{H}}_u^{(0)} \mathbf{A}_u = \text{diag} \left\{ \bar{\mathbf{H}}_{u,1}^{(0)} \left[\mathbf{F}_{N_c}^H (\mathbf{c}_u \otimes \mathbf{I}_P) \otimes \mathbf{T}_{K,L} \right], \dots, \bar{\mathbf{H}}_{u,N_b}^{(0)} \left[\mathbf{F}_{N_c}^H (\mathbf{c}_u \otimes \mathbf{I}_P) \otimes \mathbf{T}_{K,L} \right] \right\}. \quad (14)$$

Additionally, $\bar{\mathbf{H}}_{u,b}$ can be expressed as [18]

$$\bar{\mathbf{H}}_{u,b}^{(0)} = \mathbf{I}_{N_c} \otimes \bar{\mathbf{H}}_{u,b}^{(0)} + \mathbf{J}_{N_c} \otimes \bar{\mathbf{H}}_{u,b}^{(1)} \quad \forall b \in [1, N_b] \quad (15)$$

where $\bar{\mathbf{H}}_{u,b}^{(0)}$ and $\bar{\mathbf{H}}_{u,b}^{(1)}$ are both $(K+L) \times (K+L)$ channel matrices having the same structures as $\mathbf{H}_{u,b}^{(0)}$ and $\mathbf{H}_{u,b}^{(1)}$, respectively. Consequently, we have

$$\begin{aligned} \bar{\mathbf{H}}_{u,b}^{(0)} \left[\mathbf{F}_{N_c}^H (\mathbf{c}_u \otimes \mathbf{I}_P) \otimes \mathbf{T}_{K,L} \right] \\ = \left[\mathbf{F}_{N_c}^H (\mathbf{c}_u \otimes \mathbf{I}_P) \right] \otimes \left(\bar{\mathbf{H}}_{u,b}^{(0)} \mathbf{T}_{K,L} \right) \end{aligned} \quad (16)$$

where we used the fact that $\bar{\mathbf{H}}_{u,b}^{(1)} \mathbf{T}_{K,L} = \mathbf{0}_{K+L,K}$. Denoting the $(K+L) \times K$ lower-triangular Toeplitz matrix $\bar{\mathbf{H}}_{u,b} := \bar{\mathbf{H}}_{u,b}^{(0)} \mathbf{T}_{K,L}$ then gives rise to

$$\begin{aligned} \bar{\mathbf{H}}_u^{(0)} \mathbf{A}_u &= \left[\mathbf{F}_{N_c}^H (\mathbf{c}_u \otimes \mathbf{I}_P) \otimes \mathbf{I}_{K+L} \right] \\ &\quad \times \text{diag} \left\{ \mathbf{I}_P \otimes \bar{\mathbf{H}}_{u,1}, \dots, \mathbf{I}_P \otimes \bar{\mathbf{H}}_{u,N_b} \right\} \\ &= \left[\mathbf{F}_{N_c}^H (\mathbf{c}_u \otimes \mathbf{I}_P) \otimes \mathbf{I}_{K+L} \right] \bar{\mathbf{H}}_u. \end{aligned} \quad (17)$$

REFERENCES

- [1] G. R. Aiello and G. D. Rogerson, "Ultra-wideband wireless systems," *IEEE Microw. Mag.*, vol. 4, no. 2, pp. 36–47, Jun. 2003.
- [2] N. Al-Dhahir and A. H. Sayed, "The finite-length multi-input multi-output MMSE-DFE," *IEEE Trans. Signal Process.*, vol. 48, no. 10, pp. 2921–2936, Oct. 2000.
- [3] J. Balakrishnan, A. Batra, and A. Dabak, "A multi-band OFDM system for UWB communication," in *Proc. IEEE Conf. Ultra-Wideband Syst. Technol.*, Reston, VA, Nov. 2003, pp. 354–358.
- [4] *Multi-Band OFDM Physical Layer Proposal*, IEEE 802.15-03/267r5, IEEE P802.15 Working Group for WPAN.
- [5] A. Batra, J. Balakrishnan, and A. Dabak, "Multi-band OFDM: A new approach for UWB," in *Proc. Int. Symp. Circuits Syst.*, Vancouver, BC, Canada, May 2004, vol. 5, pp. 365–368.
- [6] *Channel Modeling Subcommittee Report Final*, IEEE P802.15-02/368r5-SG3a, IEEE P802.15 Working Group for WPAN, Nov. 2002, auth. J. R. Foerster.
- [7] J. R. Foerster, "The performance of a direct-sequence spread ultra wideband system in the presence of multipath, narrowband interference, and multiuser interference," in *Proc. IEEE Conf. Ultra-Wideband Syst. Technol.*, Baltimore, MD, May 2002, pp. 87–92.
- [8] Z. Liu, Y. Xin, and G. B. Giannakis, "Linear constellation precoding for OFDM with maximum multipath diversity and coding gains," *IEEE Trans. Commun.*, vol. 51, no. 3, pp. 416–427, Mar. 2003.
- [9] X. Ma and G. B. Giannakis, "Full-diversity full-rate complexity-field space-time coding," *IEEE Trans. Signal Process.*, vol. 51, no. 11, pp. 2917–2930, Nov. 2003.
- [10] C. L. Martret and G. B. Giannakis, "All-digital impulse radio for wireless cellular systems," *IEEE Trans. Commun.*, vol. 50, no. 9, pp. 1440–1450, Sep. 2002.
- [11] B. M. Sadler and A. Swami, "On the performance of UWB and DS-spread spectrum communication systems," in *Proc. IEEE Conf. Ultra-Wideband Syst. Technol.*, Baltimore, MD, May 2002, pp. 289–292.
- [12] R. A. Scholtz, "Multiple access with time-hopping impulse modulation," in *Proc. MILCOM Conf.*, Boston, MA, Oct. 1993, pp. 447–450.
- [13] Z. Wang and G. B. Giannakis, "Wireless multicarrier communications: Where Fourier meets Shannon," *IEEE Signal Process. Mag.*, vol. 17, no. 3, pp. 29–48, May 2000.
- [14] —, "Complex-field coding for OFDM over fading wireless channels," *IEEE Trans. Inf. Theory*, vol. 49, no. 3, pp. 707–720, Mar. 2003.
- [15] P. I. Withington and L. W. Fullerton, "An impulse radio communications system," in *Proc. Int. Conf. Ultra-Wide Band, Short-Pulse Electromagn.*, Brooklyn, NY, Oct. 1992, pp. 113–120.
- [16] P. Xia, S. Zhou, and G. B. Giannakis, "Bandwidth- and power-efficient multicarrier multiple access," *IEEE Trans. Commun.*, vol. 51, no. 11, pp. 1828–1837, Nov. 2003.

- [17] Y. Xin, Z. Wang, and G. B. Giannakis, "Space-time diversity systems based on linear constellation precoding," *IEEE Trans. Wireless Commun.*, vol. 2, no. 2, pp. 294–309, Mar. 2003.
- [18] L. Yang and G. B. Giannakis, "Multi-stage block-spreading for impulse radio multiple access through ISI channels," *IEEE J. Sel. Areas Commun.*, vol. 20, no. 9, pp. 1767–1777, Dec. 2002.
- [19] —, "Digital-carrier multi-band user codes for baseband UWB multiple access," *J. Commun. Netw.*, vol. 5, no. 4, pp. 374–385, Dec. 2003.
- [20] S. Zhao, H. Liu, and S. Mo, "Performance of a multi-band ultra-wideband system over indoor wireless channels," in *Proc. IEEE Consum. Commun. Netw. Conf.*, Las Vegas, NV, Jan. 2004, pp. 700–702.



Liuqing Yang (M'04) received the B.S. degree in electrical engineering from Huazhong University of Science and Technology, Wuhan, China, in 1994, and the M.Sc. and Ph.D. degrees in electrical and computer engineering from the University of Minnesota, Minneapolis, in 2002 and 2004, respectively.

Since August 2004, she has been an Assistant Professor with the Department of Electrical and Computer Engineering, University of Florida, Gainesville. Her research interests include communications, signal processing, and networking. Her

general interests include communications and signal processing, communications theory and networking. Currently, her research focuses on ultra-wide band wireless communication systems, diversity techniques for conventional communication systems and distributed and cooperative wireless networks, synchronization and channel estimation, multiple access, space-time coding, and single- and multi-carrier systems.

Dr. Yang was the recipient of the Best Dissertation Award in the Physical Sciences and Engineering from the University of Minnesota.



Georgios B. Giannakis (F'97) received the Diploma in electrical engineering from the National Technical University of Athens, Athens, Greece, in 1981, and the M.Sc. degrees in electrical engineering in 1983 and mathematics in 1986, and the Ph.D. degree in electrical engineering in 1986 from the University of Southern California (USC), Los Angeles, CA.

After lecturing for one year at USC, he joined the University of Virginia in 1987, where he became a Professor of Electrical Engineering in 1997. Since 1999 he has been a Professor with the Department of

Electrical and Computer Engineering, University of Minnesota, Minneapolis, where he now holds an ADC Chair in Wireless Telecommunications. His general interests span the areas of communications and signal processing, estimation and detection theory, time-series analysis, and system identification—subjects on which he has published more than 220 journal papers, 380 conference papers, and two edited books. Current research focuses on transmitter and receiver diversity techniques for single- and multiuser fading communication channels, complex-field and space-time coding, multicarrier, ultra-wideband wireless communication systems, cross-layer designs, and sensor networks.

Dr. Giannakis is the (co)recipient of six paper awards from the IEEE Signal Processing (SP) and Communications Societies (1992, 1998, 2000, 2001, 2003, 2004). He received Technical Achievement Awards from the SP Society in 2000 and EURASIP in 2005. He served as Editor-in-Chief for the IEEE SIGNAL PROCESSING LETTERS, as Associate Editor for the IEEE TRANSACTIONS ON SIGNAL PROCESSING and the IEEE SIGNAL PROCESSING LETTERS, as Secretary of the SP Conference Board, as Member of the SP Publications Board, as Member and Vice-Chair of the Statistical Signal and Array Processing Technical Committee, as Chair of the SP for Communications Technical Committee, and as a Member of the IEEE Fellows Election Committee. He has also served as a Member of the IEEE-SP Society's Board of Governors, the Editorial Board for the PROCEEDINGS OF THE IEEE, and the Steering Committee of the IEEE TRANSACTIONS ON WIRELESS COMMUNICATIONS.